Wind turbine wake characterization in complex terrain via integrated Doppler lidar data from the Perdigão experiment

Wind turbine wake characterization in complex terrain via integrated Doppler lidar data from the Perdigão experiment

R.J. Barthelmie[1], S.C. Pryor[2], N. Wildmann[3] and R. Menke[4]

[1]Sibley School of Mechanical and Aerospace Engineering, Cornell University (CU), USA
[2]Department of Earth and Atmospheric Sciences, Cornell University (CU), USA
[3]Institute of Atmospheric Physics, Deutsches Zentrum für Luft- und Raumfahrt (DLR), Germany
[4]Wind Energy Department, Technical University of Denmark (DTU), Denmark

rb737@cornell.edu

Abstract. During the intensive period (May-June 2017) of the Perdigão experiment, three sets of Doppler lidar were operated to scan the wake of the wind turbine (WT) on the southwest ridge. CU operated a Doppler scanning lidar in the valley bottom approximately 1 km northeast of the WT and conducted multiple arc scans and two RHI scans every 10-minutes centred on the WT. DTU used a dual Doppler lidar system scanning almost horizontally from the northeast ridge. Two of the three DLR lidars were in-plane with the WT for the main wind direction, one in the valley and one on the distant mountain ridge. The third DLR lidar was on the southwest ridge. All three systems (CU, DTU and DLR) were operated such that in data processing vertical and/or horizontal profiles of the wake can be derived at different distances from the WT. The paper describes the strategies used to scan the wake by the three groups and compares wake characteristics derived from the different systems.

1 Introduction

Power losses and enhanced loads due to wind farm wakes (including the 'deep array' effect and array-array interactions) are typically largest in offshore wind farms [1, 2]. Most experiments designed to characterize individual wind turbine wakes have been conducted onshore to allow use of lidar [3, 4] to measure the 3-dimensional (3d) flow field. Despite significant progress in recent years it has proved complex to extract quantitative (and robust) metrics of wakes such as length scales and velocity deficit [5] because of the complexity of the phenomena (e.g. dependence of wake behaviour on the turbine itself, the wind farm layout and atmospheric characteristics [2, 6]) and challenges in defining optimal lidar scan strategies and effective integration of data from different remote sensing platforms [7]. These issues of wake characterization are amplified in complex terrain, in part because of the complexity of flow such as turning, recirculation zones and waves that both make describing the inflow/freestream very challenging [8], and in the wake behaviour itself which responds to the terrain slope as well as the flow [9-11]. While numerical models have been applied to examine wakes in complex terrain [12, 13], the objective of this work is to describe wake measurements with lidars within the Perdigão experiment and to evaluate the benefits of using multiple lidars/different scanning strategies to provide a more accurate, precise and detailed set of wake characteristics.

2 Experiment design

2.1 The Perdigão experiment

The overarching objective of the Perdigão experiment [14] is to provide a high-quality, high-resolution data set describing flow in complex terrain using observations derived from multiple measurement platforms. The site is a double-ridge extending for several kilometres with hilltop heights up to 300 m above the local terrain [10]. For the long-term experiment January-July 2017, multiple meteorological masts with heights up to 100 m were installed across the domain and an array of Doppler lidars (including those from CU and DTU) were operated. For the intensive operating phase (IOP) (May-June 2017) a vast array of additional instruments was installed including further Doppler lidars. Data and instruments described here are focused on understanding the characteristics and behaviour of the wake from a single wind turbine (WT) on the southwest ridge (Figure 1). Three groups (CU, DLR, DTU) operated Doppler lidars that include wake measurements (Table 1, Figure 1). In order to develop the framework and evaluate the benefits of integration of multiple independent measurements, a test case of a two-hour period (26 May 2017, 21:00 to 23:00 UTC) in which all instruments were measuring with their most suitable scanning strategy for a joint wake detection is analysed herein. This period features a WT wake embedded in a stable nocturnal boundary layer (Figure 2).

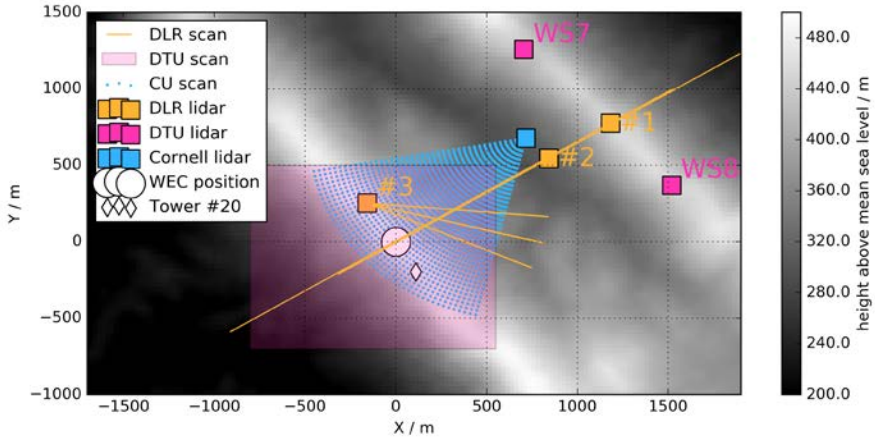

Figure 1: The topography of Perdigão with the location of Doppler lidars used for wake measurements (CU, DTU, DLR) and their scans highlighted. For the DTU scans, only the overlapping region for the dual Doppler retrieval is marked. The wind turbine (WEC) is located on the SW ridge.

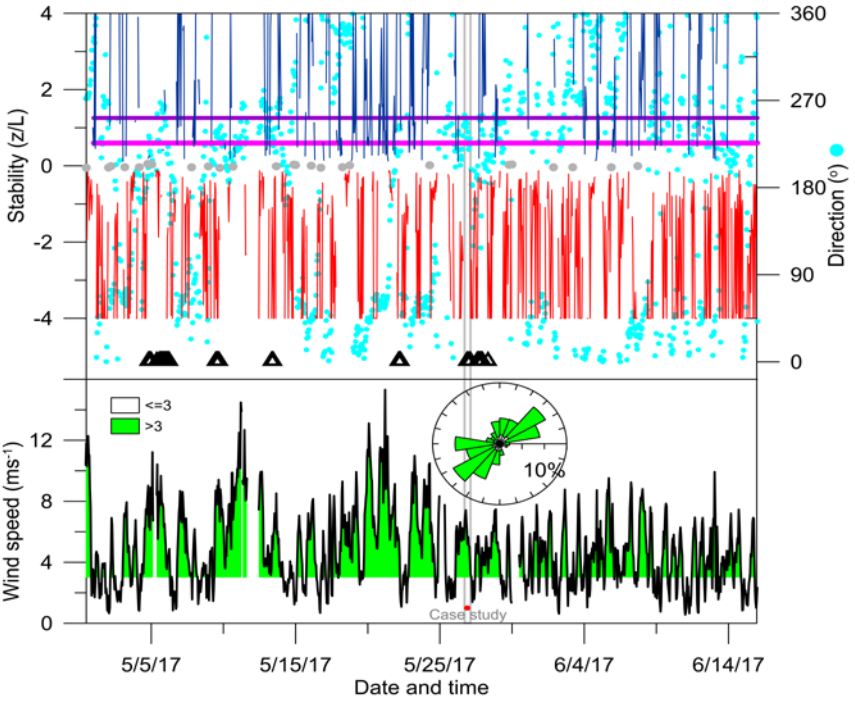

Figure 2: Overview of the conditions during the IOP. Wind speeds (>3 ms^{-1} shaded green) and direction are from Tower 20. Stability is calculated as *z/L* where red lines = unstable conditions, blue lines = stable conditions and grey dots = near-neutral conditions. Periods with all lidar systems operating are shown by the black triangles. The period of the case study 21:00 UTC to 23:00 UTC on 26 May 2017 is indicated by the grey box.

2.2 Scanning strategies

Table 1 summarizes the primary features of the lidars used in this study along with the scan strategies.

Table 1. Overview of the scanning Doppler lidar WT wake measurements. Positions are shown relative to the WT location and heights relative to WT hub-height.

Lidar	Unit	DLR #1	DLR #2	DLR #3	DTUWS7	DTUWS8	CU42
Position X	m	1183	843	-158	705.5	1519.5	717
Position Y	m	776	544	252	1256.6	369.2	676
Position Z	m	-103	-239	-82	-124.8	-108	-244
Scan type		RHI	RHI	RHI 3 az angles	quasi-horizontal	quasi-horizontal	arc, RHI, VAD
Frequency C= continuous		C	C	C	10min per ½ hour	10min per ½ hour	C
Azimuth, min	deg	236.9	236.9	95,105,115	183.5	221.2	193.5
Azimuth, max	deg	236.9	236.9	95,105,115	246.8	279.4	259.5
Elevation, min	deg	-8	8	-2	3.4	3.1	9
Elevation, max	deg	100	160	50	5.6	4.8	23
Accumulation time	ms	1000	500	500	500	500	1000
Angular Speed	deg/s	1	2	1	0.7	0.7	~1.5
Duration of scan	s	108	76	52	50	50	603.5
Range gate min	m	100	50	50	700	700	60
Range gate max	m	2500	1400	1000	2640	2640	1230
Range gate separation	m	20	10	10	10	10	30
Pulse Length	ns	200	100	100	200	200	200
FFT points		128	64	64	64	64	N/A
Physical Resolution	m	50	25	25	35	35	60

2.2.1 CU

The CU Galion lidar scans [15] were designed to capture the 3d volume of the WT wake over a relatively large area (shown in Figure 1). Each 10-minute scan geometry comprised:

- Telescoping arc scans with closer spacing near the WT centreline (980 m, 226° from the Galion) in both the horizontal and vertical (Figure 3(a)-(k)). These were used to maximize the coverage of the WT wake for that direction but permit wake tracking for a wide swath of wind directions.
- Two detailed Range Height Indicator (RHI) scans close to the wake centreline (Figure 3(j)).
- Three Vertical Azimuth Display (VAD) scans that were used for initial estimation of the wind direction at the wind turbine hub-height (WTHH) for identification of possible wake cases (Figure 3 panel (l)). The ultimate freestream wind speed and direction was derived using the arc scans.

2.2.2 DLR

The DLR deployed three long-range Leosphere Windcube 200S Doppler lidars [16]. Lidar #1 and lidar #2 conducted RHI scans in a coplanar configuration that can be combined to calculate the wind vector in two dimensions in the vertical scanning plane (Figure 4) and thus examine wake propagation along the main wind direction [17]. From 22 May (including the case study), lidar #1 experienced problems with the data acquisition board causing intermittent corruption of wind data. Thus, the coplanar retrieval could not be run continuously and wake detection presented relies solely on the radial wind speed measurements of lidar #2. On 26 May, lidar #3 measured RHIs at three distances from the WT (Figure 1) to identify the lateral displacement of the wake with respect to the coplanar scans and show the change of the wake width with distance. RHIs of all DLR lidars intersect at three locations at approximately 2.5, 3.5 and 4.5D (D = rotor diameter) from the WT to allow retrieval of vertical profiles of mean horizontal wind speed and wind direction (at ‘virtual towers’) [18].

2.2.3 DTU

Two DTU WindScanners [15], modified Leosphere Windcube 200S scanning lidars, were located on the northeast ridge and performed horizontal scans along the southwest ridge following a line 80 m above the ridge-top height. Thus, the two scanners measured at an average elevation of 4.3° from the horizontal plane. In an area (1350 m x 1200 m) centred around the WT dual-Doppler retrievals are available and horizontal wind speeds are calculated (see Figure 5, left). This configuration allows tracking of the wake up to 800 m downstream depending on the wind direction and the vertical wake displacement. This scanning strategy was pursued every half hour for ten minutes and determines the time periods for the joint wake centre detection in the following.

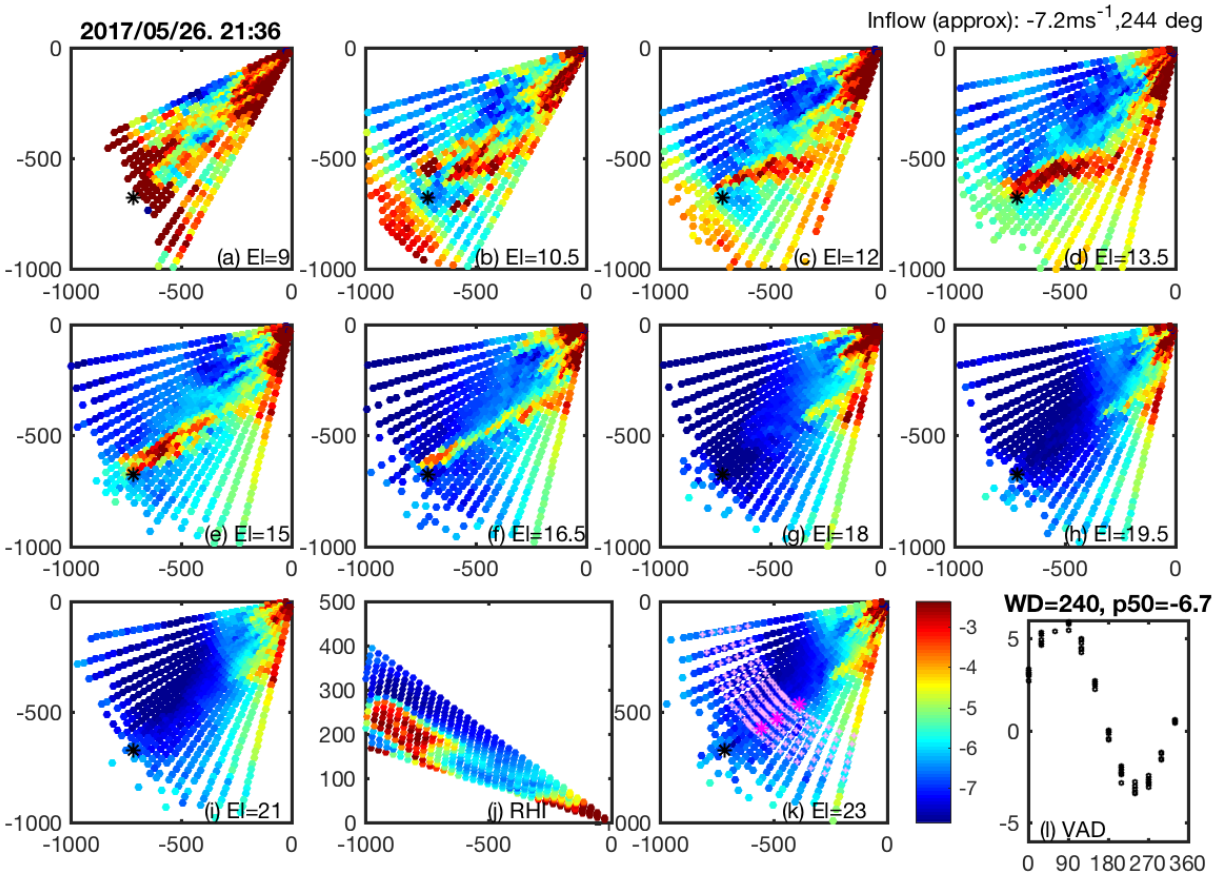

Figure 3: An example of line-of-sight (LoS) velocities (in ms^{-1} indicated by the colour bar) on 26 May 2017 at 21:46-21:56 UTC as measured by the CU scanning Doppler lidar located at (0,0) almost 1000 m northeast of the WT (indicated by the black *). Panels (a-i) and (k) show arc scans at different elevation angles (indicated lower right, e.g. El=9 is elevation angle of 9°). Panel (j) shows a RHI vertical slice along a direction of 226°. In panel k (El=23) the downwind distances (2, 2.5, 3.0, 3.5, 4 and 4.5 D, recall D = WT rotor diameter) at which 2d planar slices through the wake are shown in magenta dashed lines. The three * indicate the locations of the DLR virtual towers. Panel (l) shows the wind speed and direction retrieved from three VAD scans at the WTHH that are used for preliminary determination of direction. Inflow LoS velocity and direction shown in Figure 6, are determined from arc scans at the WTHH and distance.

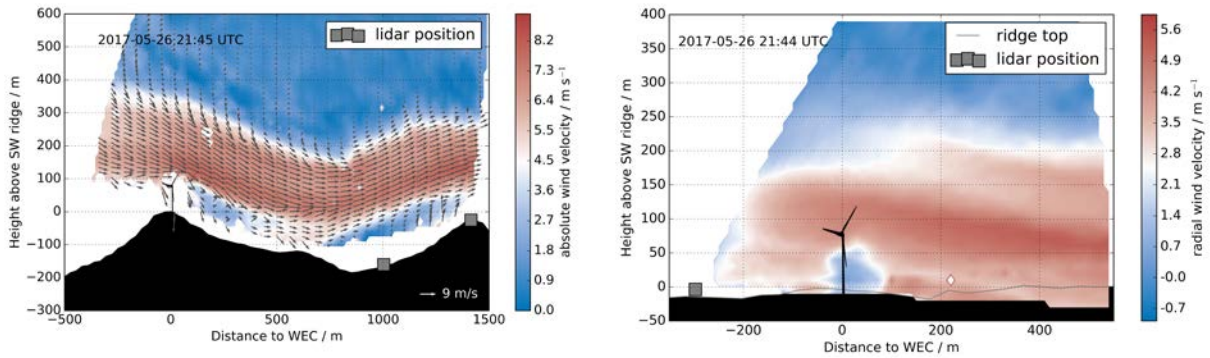

Figure 4: Measurements from the DLR scanning Doppler lidars on 26 May 2017, averaged from 21:40 to 21:50 UTC. On the left, the result of a coplanar scan with retrieval of horizontal and vertical wind speeds. On the right, a RHI cut through the wake at approximately 2.5 D downstream, projected onto a plane parallel to the ridge is shown for the same time average.

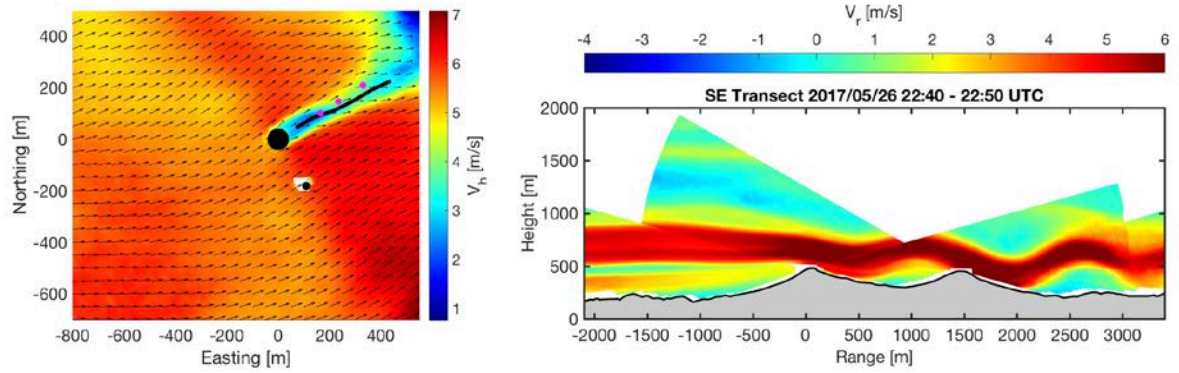

Figure 5: Measurements from DTU's WindScanners on 26 May 2017 averaged from 22:40 to 22:50 UTC. Left: Horizontal wind speeds (V_h) showing the WT wake and tracking to 6 D downstream using a Gaussian fit method. The magenta circles indicate DLR's virtual towers, the black circle shows the WT position, the smaller black circle indicates the position of Tower #20. Right: A composite of radial wind speeds (V_r) of four scanning lidars, measuring a vertical plane perpendicular to the ridges and illustrating the presence of a terrain following low-level jet (wind direction is from the left).

3 Wake detection and location

The different scanning strategies employed present an opportunity to explore ways to optimally integrate the resulting data and maximise the information extracted from the multiple lidar systems. Normally to determine wake characteristics in flat terrain, the coordinates can be rotated to align the wake centre allowing features such as the wake width, centre [19], meander etc to be relatively straightforward to compute [20] but this approach is difficult to apply in complex flow environments. While a freestream wind speed can be indicated using data from the sonic anemometer on Tower 20 at 78 m height (6.0 ms^{-1} and 246° at 21:00 UTC, 26 May), it is not representative of the background wind speed over the valley (Figure 3 and 4). Similarly, the ridge feature introduces turning (Figure 5) and these make determining the freestream field challenging. Below we describe the methods used for wake tracking from the individual systems.

3.1 CU

As indicated by Figure 6 the wake centre is objectively identified from the CU Galion scans on 2d vertical planes at distances from the WT of 2, 2.5, 3, 3.5, 4, 4.5 D (Figure 3, panel j). To account for the complexity of the background flow, the anomaly of the velocity field at each point is computed from the mean in 20-m heights increments and used to detect the wake. The wake centre is determined as the location of the minimum velocity starting the search from the location if the wake propagated

on a horizontal plane (shown as the black square in the upper left frame of Figure 6). Figure 6 shows the location of the wake centre in black (o) from the observations and in magenta from the interpolated velocity field (using cubic spline). As shown, this technique detects the centre of the non-symmetric wake and tracks it as it moves down the slope.

Thus, the methods used to determine the wake characteristics (location in the x, y, z-planes and velocity deficit along with wake asymmetry) from the Galion are: i) a minimum in the observed LoS anomaly from the height-corrected background wind field ii) the same method but on the wind field interpolated using a cubic spline iii) by fitting a Gaussian curve to the LoS velocity deficit (see examples in Figure 7). The Gaussian fit is generally a more a successful fit in the horizontal plane than in the vertical, probably because vertical shear creates a non-Gaussian profile.

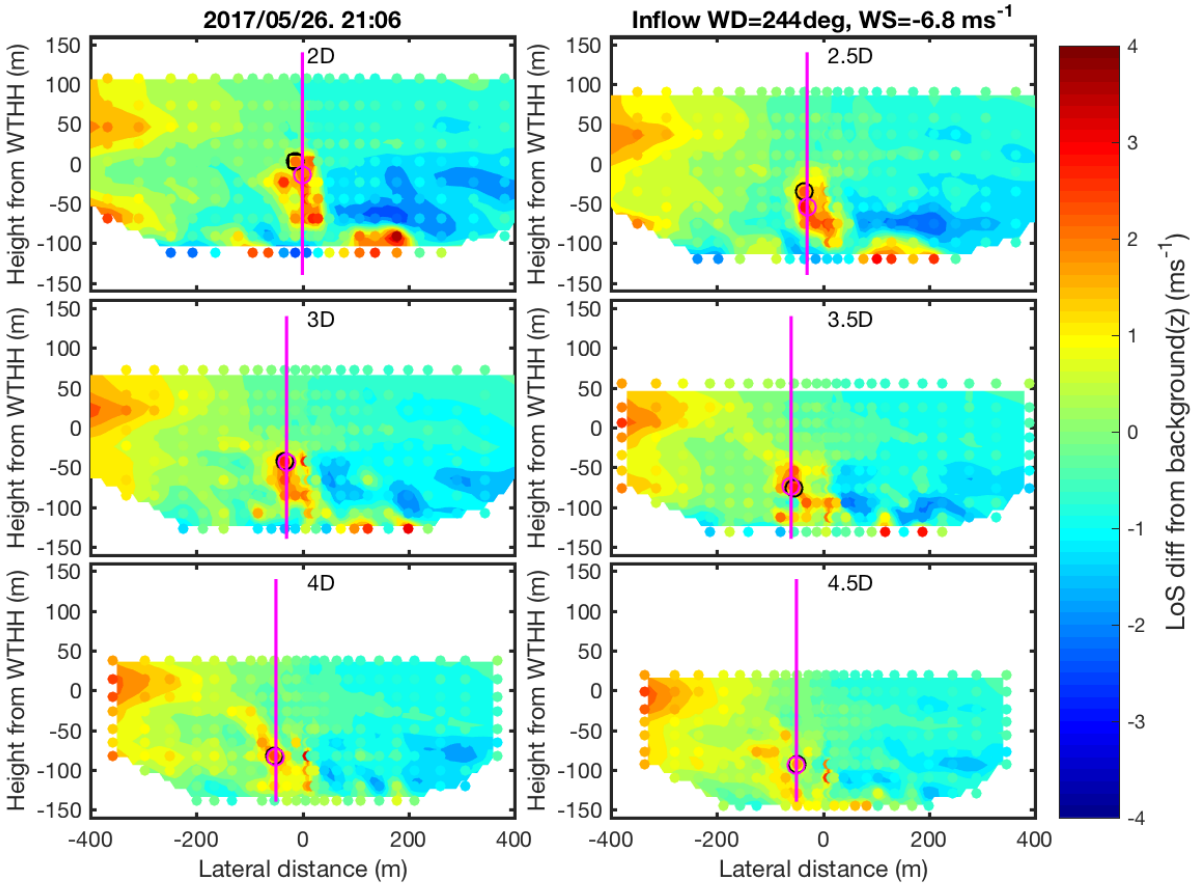

Figure 6: Vertical slices of LoS velocity anomaly determined as the difference of observed velocity at each scanned point to the background field at that height (Obs=small solid coloured circles) or for a field interpolated (coloured contours) using cubic spline (Int) for different distances 2, 2.5 D etc. from the WT. Heights are shown relative to the WT hub-height (78 m above the ridge). The black square in the first panel indicates the centre determined from the first estimate of the wind direction from the VAD scans. The black circles indicate the wake centre from the observations and the magenta circle the wake centre from the interpolated field. The magenta-dashed vertical lines indicate the location of the vertical slices along the line of sight shown in Figure 7.

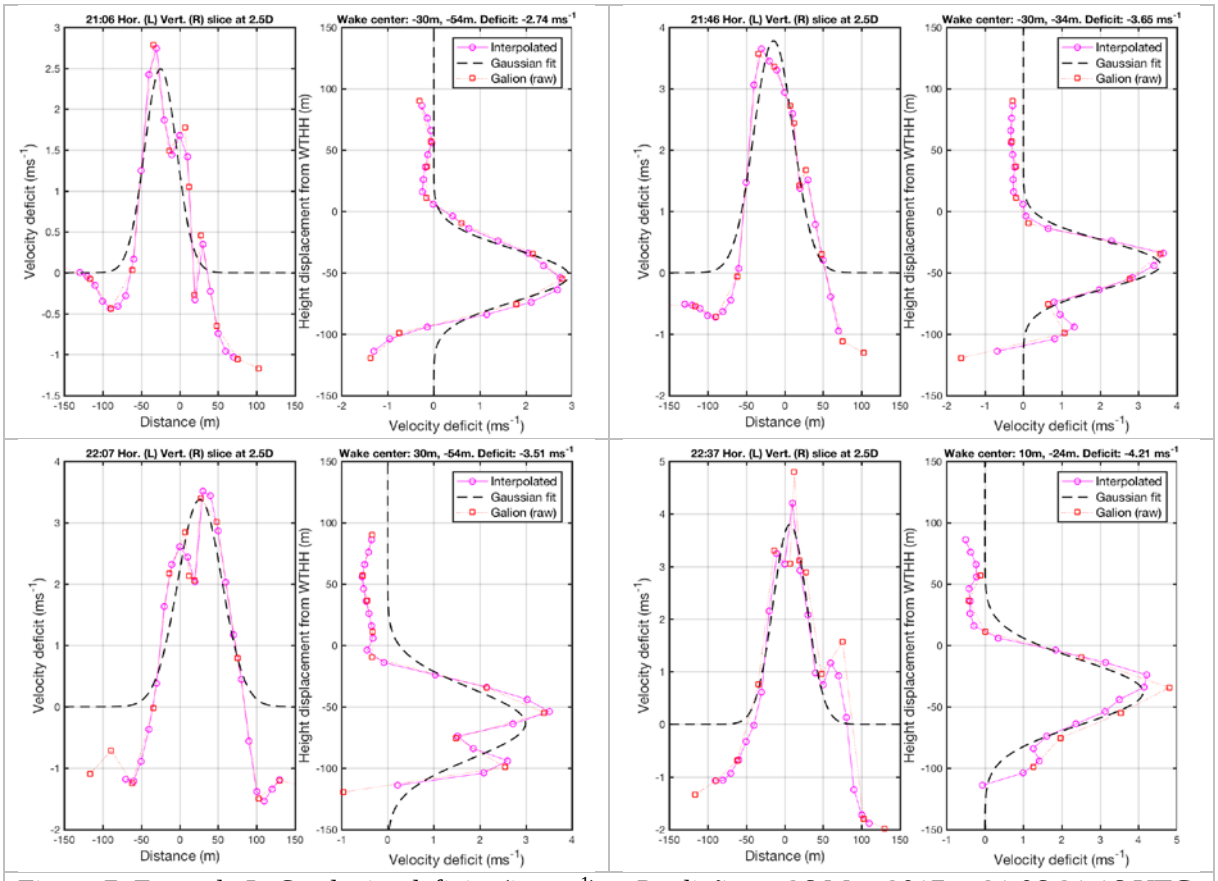

Figure 7: Example LoS velocity deficits (in ms^{-1}) at Perdigão on 26 May 2017 at 21:06-21:16 UTC, 21:46-21:56, 22.07-22:17 and 22:37-22:47 UTC at 2.5 D. For each of the four times, the left panel shows a horizontal slice through the wake and the right panel a vertical slice. The red lines are points observed by the CU Galion, pink lines indicate the wake from the interpolated mesh-grid and the black line is from a Gaussian fit. The values above the right-hand panel in each frame shows the location of the wake centre (horizontal displacement from a direct centreline and vertical displacement from the WTHH), plus the velocity deficit.

3.2 DLR

To detect the wake centre from RHI scans of lidar #2, the radial wind speed measurements were interpolated to a regular grid with a spacing of 10 m. Starting from 40 m (0.5D) downstream of the WT, vertical profiles of wind speeds from 100 m below to 100 m above hub height are fitted to a Gaussian function. If a wake is detected, the detection is continued for the next vertical profile downstream, using the detected wake centre, width and amplitude as the initial guess for the succeeding Gaussian fit. Criteria for a successful fit of a Gaussian function are that the centre of the Gaussian is within the bounds of the vertical profile, the amplitude (i.e. wind speed deficit) is not larger than the incoming flow, the standard deviation (i.e. width of the wake) is not larger than 300 m and the wake centre location does not deviate more than 20 m from the preceding. Figure 8 (left) shows the result for a case where the wake follows the flow into the valley but then gets lifted and develops a wavy propagation path. For the measurements of lidar #3, the detection of wake centres is considerately more difficult, because the wake is seen as a two-dimensional structure with time varying shape. Additionally, the wake was diverted into the valley so far that the whole shape could not be covered with the lowest elevation angles of the RHI scans. Nevertheless, a detection of the wake has been performed with a two-dimensional Gaussian function and Figure 8 (right) shows one case of a good detection.

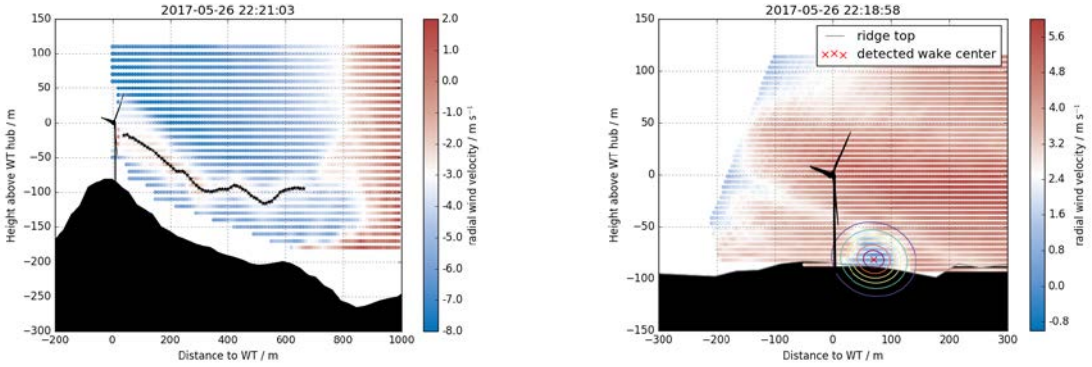

Figure 8: Examples of wake centre detection from DLR. Left: detected wake centres (indicated as black stars) from RHI scans of lidar #2 from 0.5 to 9D. Right: A two-dimensional wake centre detection from an RHI of lidar #3 at 3.5D at approximately the same time. The red cross marks the wake centre and the contour lines visualize the shape of the detected Gaussian function.

3.3 DTU

Data from the DTU WindScanners are used to derive the u and v component of wind at high temporal and spatial resolution. The wake centre is tracked using a Gaussian fit along profiles that are orientated perpendicular to the wind direction measured by tower 20. The profiles are positioned 1-6 D downstream of the WT. This algorithm works well to determine the horizontal location of the wake centre. However, the wake is frequently displaced in the vertical (in this case it was terrain following) (Figures 3, 8), thus in some periods the wake can only be tracked up to two 2 D downstream. Figure 5 shows a period where the horizontal location of the wake can be tracked 6 D downstream. However, the wake is not necessarily centred on the measurement plane making it difficult to determine the absolute velocity deficit.

4 Initial integration of the wake characterization results

There are many challenges in detection and characterization of WT wakes in complex terrain. Flow inhomogeneity increases uncertainty in the measurements due to the relatively large scanning volumes of lidar. Our initial integration has focused on tracking of the wake centre at different distances downwind. Independent estimates of the WT wake location from each group are summarized in Figure 9 for the four ten-minute periods between 21:00 and 23:00 when horizontal dual-Doppler scans are available. As shown, all three lidar systems show consistent directions of the wake advection and also that in this two-hour period the wake centre is terrain following. The DTU results are for the near-wake near-horizontal plane and show a slightly more southerly trajectory. The CU high arc scans show the wake centre from the Galion data sampled to reproduce the DTU horizontal scan and are consistent with the DTU scans. The wake centre locations determined from the CU scans sampled to retrieve wake locations on a horizontal plane at WTHH (i.e. approximately mimicking the DTU scans) and following the wake at discrete distances downstream indicate some differences in terms of the wake location. This reflects both the challenges in identifying the wake location when the centreline is displaced from the horizontal and also the asymmetry of the wake. In cross-sectional view, the wake centre detections of CU and DLR lidar #2 and #3 are shown. The wake centre for all four cases is always below the DTU scanning plane which suggests that the top of the wake is deflected south while the lower part stays in the plane or propagates to the north as suggested by the CU detection algorithm. The longest wakes are detected at 21:10-21:20 with clear Gaussian-shaped profiles up to 9 D downstream.

Since the wake shape is highly asymmetric (Figure 6), the differences between the wake centre location shown in Figure 9 may be attributable to both the differences in technique used to identify the wake centre and the differences in the scan types. Nevertheless, the results are promising and are beginning to evolve a clearer picture of the degree of closure it is possible to achieve and what

additional information regarding the wake characterization can be yielded by integration data from independently operated remote sensing systems.

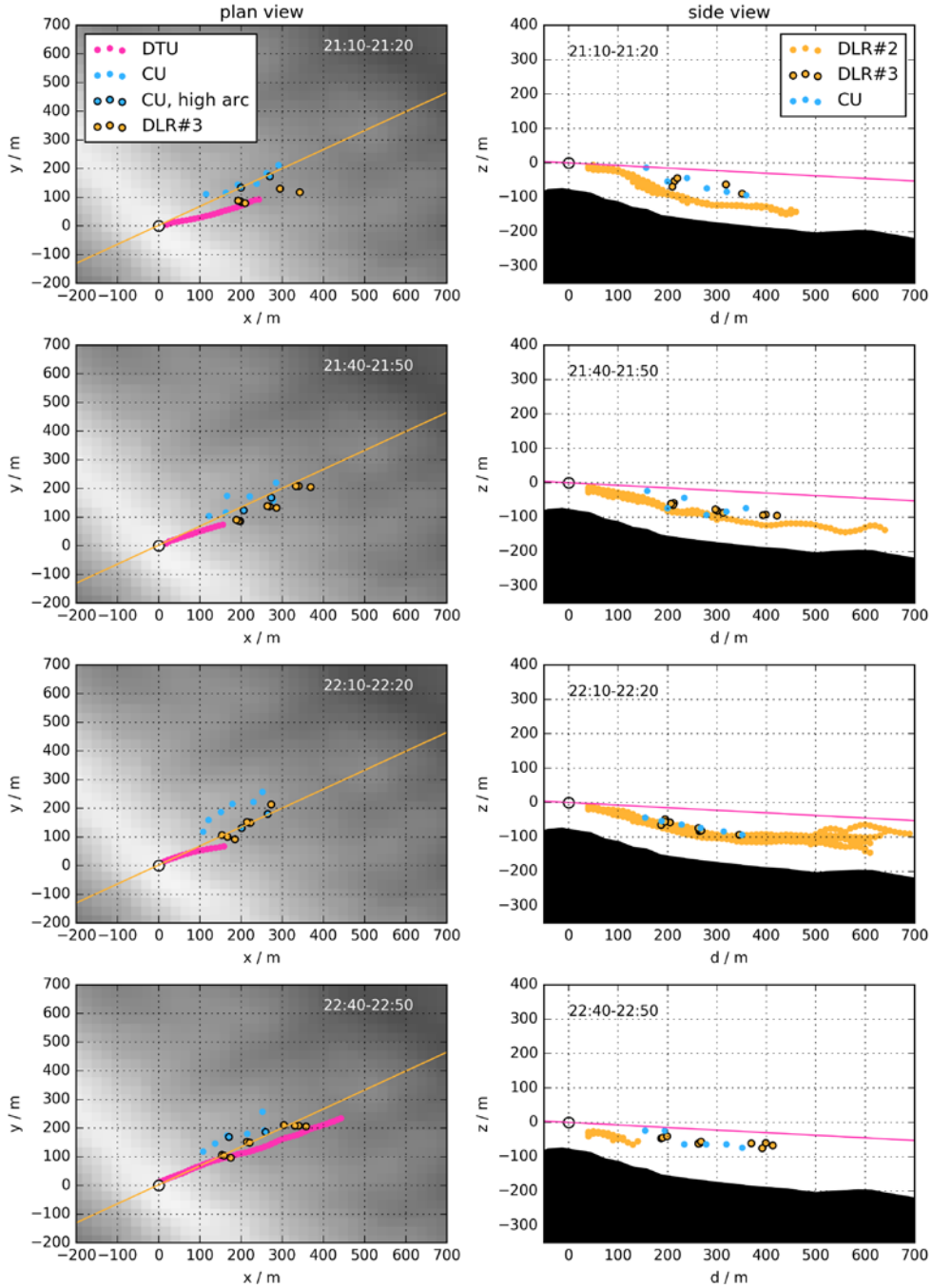

Figure 9. Wake centre position using data from 26 May 2017 from 21:10-21:20, 21:40-21:50, 22:10-22:20 and 22:40-22:50 from the three lidar systems. The left column shows the plan view, the right column shows the side-view. In the plan view, the scanning plane of DLR lidars #1 and #2, which is also used as the projection plane for the side view, is indicated by the yellow line. In the side-view the DTU scanning plane with 4.3° elevation is indicated with a pink line. Two sets of results are shown in the left panels for CU and reflect the wake centre position at the DTU scan elevation (CU, high arc) and from the cross-section such as that shown in Figure 6.

5 Summary and future work

The Perdigão experiment has presented one of the first opportunities to measure WT wakes with lidar in highly complex terrain and to investigate the benefits of integrating data from different lidar and scanning strategies. While this has proved complicated, due in part to logistical issues that reduced the availability of some scans during the IOP, there are also obvious advantages to be gained from integrating the scans. While the DTU scans provide high temporal and spatial resolution giving good indication of the acceleration and turning of the flow at the ridge, the use of the near-horizontal plane means that wakes that are terrain following can only be tracked over a relatively short distance. DLR used RHI scans allowing the wake centre to be tracked as it moved down the slope but losing the centre if there was significant turning. The Galion scanning strategy covers a large horizontal and vertical area but with the cost of reduced temporal resolution.

We have illustrated the first steps in the process of the integration of these datasets as we work to identify common temporal and spatial frameworks that can be utilized for different scans. Since none of the instruments were co-located, this proved complex since the wake centre lines were different and, given turning at the ridge and wake meander in the valley, no coordinate rotation was possible. While the wake centres have been located we need to identify why they are not identical and whether this is due to wake asymmetry, the scan type or the detection methods. Following this, the next steps are to identify common methods for further wake metrics such as wake width and wind speed deficit. It needs to be evaluated if they can be derived from the different scan types and whether it is optimal to use LoS wind speeds (as DLR and CU) or wind components as DTU. Integration of the datasets will permit an assessment of whether using different types of lidars/scan types can reduce the uncertainty in the quantified wake characteristics.

6 References

[1] Barthelmie, RJ, et al. J Atmos Oceanic Tech, 2010. **27**(8): 1302.
[2] Barthelmie, RJ, KS Hansen & SC Pryor. Proc IEEE, 2013. **101(4)**: 1010.
[3] Iungo, GV, Y-T Wu, & F Porté-Agel. J Atmos Oceanic Tech, 2013. **30**(2): 274.
[4] Lundquist, JK, MJ Churchfield, S Lee & A Clifton. Atmos Meas Tech, 2015. **8**(2): 907.
[5] Doubrawa, P, et al. Remote Sensing, 2016. **8**(939): doi:10.3390/rs8110939.
[6] Machefaux, E, et al. Wind Energy, 2016. **19**(10): 1785.
[7] Barthelmie, RJ, et al. Bull Am Meteor Soc, 2014. **95**(5): 743.
[8] Meyer Forsting, AR, A Bechmann, & N Troldborg. J Physics Conf Series 2016 **753** 032041.
[9] Politis, ES, et al. Wind Energy, 2012. **15**: 161.
[10] Vasiljević, N, et al. Atmos Meas Tech, 2017. **10**(9): 3463.
[11] Menke, R, et al. Wind Energy Science (submitted), 2018.
[12] Shamsoddin, S &F Porte-Agel. Bound Layer Meteor, 2017. **163**(1): 1.
[13] Berg, J, et al. J Physics Conf Series, 2017. **854**(1): 012003.
[14] Mann, J, et al. Phil Trans Royal Society A: 2017. **375**(2091).
[15] Barthelmie, RJ, et al. Wind Energy, 2016(19): 2271-2286 DOI: 10.1002/we.1980.
[16] Vasiljevic, N & T Gerz. Atmos. Meas. Tech. Discuss., 2018. 10.5194/amt-2018-55, in review.
[17] Wildmann, N, S Kigle, &T Gerz. J Physics Conf. Series., in review, 2018.
[18] Calhoun, R, et al. J. App Meteor Clim, 2006. **45**(8): 1116.
[19] Doubrawa, P, RJ Barthelmie, H Wang, & MJ Churchfield. Wind Energy, 2017. **20**(3): 449.
[20] Barthelmie, RJ, P Doubrawa, H Wang, & SC Pryor. J Physics Conf Series 2016 **753** 032034.

Acknowledgements

We would like to acknowledge funding from the National Science Foundation #1565505 (to CU) and the assistance of DTU, NCAR, INEGI, UPorto in establishing and running the Perdigão experiment. We also acknowledge the funding from the Federal Ministry of Economy and Energy on the basis of a resolution of the German Bundestag under the contract numbers 0325518 and 0325936A (to DLR), and the Danish Energy Agency for funding through the New European Wind Atlas project (to DTU).